

**THE EFFECT OF REINFORCED-EPOXY COATING ON THE  
BENDING MODULUS OF MICRO-CANTILEVER USING  
PHASE-SHIFT SHADOW MOIRÉ**

**LIM JIUNN HSUH**

**UNIVERSITI SAINS MALAYSIA**

**2012**

**THE EFFECT OF REINFORCED-EPOXY COATING ON THE BENDING  
MODULUS OF MICRO-CANTILEVER USING PHASE-SHIFT SHADOW  
MOIRÉ**

**by**

**LIM JIUNN HSUH**

**Thesis submitted in fulfillment of the requirements  
for the degree of  
Doctor of philosophy**



**December 2012**

Dekan/Dean  
Institut Pengajian Siswazah  
Universiti Sains Malaysia  
11800 Pulau Pinang.

**Pengisytiharan /Declaration**

Saya isytiharkan bahawa kandungan yang dibentangkan di dalam tesis ini adalah hasil kerja saya sendiri dan telah dijalankan di Universiti Sains Malaysia kecuali dimaklumkan sebaliknya.

*I declare that the contents presented in this thesis are my own work which was done at Universiti Sains Malaysia unless stated otherwise. The thesis has not been previously submitted for any other degree.*

<div style="text-align: center; margin-bottom: 10px;">  </div> <p>Tandatangan Calon (Signature of Candidate)</p> <p>Nama Calon (Name of Candidate)  <u>LIM JIUNN HSUH</u></p> <p>No. Kad Pengenalan/No. Pasport :          IC. No/Passport No. :</p> <table border="1" style="width: 100%; text-align: center; border-collapse: collapse;"> <tr> <td>7</td><td>5</td><td>1</td><td>2</td><td>0</td><td>2</td><td>0</td><td>2</td><td>5</td><td>2</td><td>7</td><td>1</td> </tr> </table> <p>Tarikh (Date) : <u>6/12/2012</u></p>	7	5	1	2	0	2	0	2	5	2	7	1	<p>Disaksikan oleh (Witnessed by) :</p> <div style="text-align: center; margin-bottom: 10px;">  </div> <p>Tandatangan Saksi (Signature of Witness)</p> <p>Nama Saksi (Name of Witness)  <u>SNG JIUNN CHIF. (DR.)</u></p> <p>No. Kad Pengenalan/No. Pasport :          IC. No/Passport No. :</p> <table border="1" style="width: 100%; text-align: center; border-collapse: collapse;"> <tr> <td>8</td><td>8</td><td>1</td><td>0</td><td>1</td><td>2</td><td>0</td><td>2</td><td>6</td><td>1</td><td>0</td><td>5</td> </tr> </table> <p>Tarikh (Date) : <u>6/12/2012</u></p>	8	8	1	0	1	2	0	2	6	1	0	5
7	5	1	2	0	2	0	2	5	2	7	1														
8	8	1	0	1	2	0	2	6	1	0	5														

Untuk kegunaan Institut Pengajian Siswazah  
For IPS use Only

Pengesahan Penerimaan oleh IPS :	Nama Staf:	Tarikh :
----------------------------------	------------	----------

## **ACKNOWLEDGEMENT**

I would like to express my gratitude and appreciation to my main project supervisor Prof. Dr. Mani Maran Ratnam, for his motivation and assistance in this project. I would like to thank for his valuable advice and supervision for this project. His expertise and recommendation played an important role in the successful completion of this project. Without his guidance, this project may not have been completed on time. Besides, I would also like to express my gratitude to Assoc. Prof. Dr. Ishak b. Hj. Abdul Azid and Assoc. Prof. Dr. D. Mutharasu, my co-supervisors for their support, advice, motivation and help in this project.

In the meantime, I would like to thank for my parents for their immeasurable love and support. For my wife, brother and sisters, I would like to thank for their unlimited moral support. Finally, thank those who have helped me in this project.

# TABLE OF CONTENTS

	<b>Page</b>
ACKNOWLEDGEMENT.....	ii
TABLE OF CONTENTS.....	iii
LIST OF TABLES.....	vi
LIST OF FIGURES.....	vii
LIST OF ABBREVIATIONS.....	xiii
LIST OF APPENDICES.....	xiv
ABSTRAK.....	xv
ABSTRACT.....	xvii
<b>CHAPTER 1 – INTRODUCTION</b>	
1.0 Research Background.....	1
1.1 Motivation of the Study.....	5
1.2 Problem Statement .....	6
1.3 Objectives of Study.....	7
1.4 Scopes of Study .....	7
1.5 Contributions .....	8
1.6 Thesis Outline.....	8
<b>CHAPTER 2 – LITERATURE REVIEW</b>	
2.0 Overview.....	11
2.1 The Application of Optical Techniques in Deflection Measurement.....	11
2.2 The Characterization Technique for Micro-structures.....	21
2.3 The Applications of Polymer Materials in MEMS.....	28
2.4 The Application of FEA in the Analysis of MEMS.....	31

2.5	The Effect of Coating to the Material Properties.....	34
2.6	Chapter Summary.....	36
<b>CHAPTER 3 – RESEARCH METHODOLOGY</b>		
3.0	Overview.....	39
3.1	Sample Preparation.....	40
3.1.1	Miniaturized copper cantilever.....	40
3.1.2	Silicon micro-cantilever.....	40
3.1.3	Reinforced-epoxy coated PET cantilevers.....	57
3.2	Experimental Setup.....	61
3.2.1	Deflection measurement of miniaturized copper cantilever.....	61
3.2.2	Deflection measurement of silicon micro-cantilever.....	63
3.2.3	Deflection measurement of reinforced-epoxy coated PET cantilever.....	65
3.3	Algorithm and Analysis.....	65
3.3.1	Principle of the shadow moiré method.....	65
3.3.2	Phase-shifting and interferogram analysis algorithm.....	73
3.3.3	Image Enhancement Technique.....	77
3.3.4	Deflection theory and determination of bending modulus.....	79
3.4	Experimental Procedures.....	83
3.4.1	Determination of scaling factor in the imaging system.....	83
3.4.2	Deflection measurement of miniaturized copper cantilever.....	85
3.4.3	Deflection measurement of silicon micro-cantilever.....	87
3.4.4	Deflection measurement on reinforced-epoxy coated PET cantilever.....	89
3.5	Finite Element Analysis of Reinforced-epoxy Coated PET Cantilever.....	90
3.5.1	Element selection.....	91

3.5.2	Modeling of reinforced-epoxy coated PET cantilevers.....	98
3.6	Chapter Summary.....	99
CHAPTER 4 – RESULTS AND DISCUSSIONS		
4.0	Overview.....	101
4.1	Deflection Measurement of Miniaturized Copper Cantilever.....	101
4.1.1	Measurement accuracy.....	107
4.2	Deflection Measurement of Silicon Micro-cantilever.....	115
4.2.1	Image enhancement.....	117
4.2.2	Deflection measurement of silicon micro-cantilever.....	120
4.2.3	The effect of using the average value of the cantilever thickness...	122
4.2.4	Determination of the measurement accuracy.....	124
4.2.5	Determination of bending modulus of cantilever material.....	135
4.2.5	Uncertainty analysis.....	139
4.3	Deflection Measurement of Reinforced-epoxy PET Micro-cantilever.....	139
4.4	Modeling of Reinforced-epoxy Coated PET Cantilevers.....	146
4.5	Chapter Summary.....	153
CHAPTER 5 – CONCLUSION AND FUTURE WORK		
5.0	Overview.....	155
5.1	Conclusions.....	155
5.2	Contribution from the Research.....	157
5.3	Limitation.....	158
5.4	Recommendation for Future Works.....	158
REFERENCES.....		160
APPENDICES		
LIST OF PUBLICATIONS		

## LIST OF TABLES

		<b>Page</b>
Table 2.1	The major features of some popular optical methods applied for displacement measurement	19
Table 2.2	The values of Young's modulus for silicon dioxide material at micro-scale conditions	22
Table 3.1	The average value of width and thickness of the reinforced-epoxy coated PET cantilever	60
Table 3.2	Phase and range of values according to values in the Numerator and the Denominator in expression for arctangent $\phi$	75
Table 4.1	The bending modulus calculated from different loads and the corresponding uncertainties	107
Table 4.2	The surface profile measured using profile projector	108
Table 4.3	The comparison among the results from optical measurement, profile projector measurement and theoretical value of the cylinder surface profile	115
Table 4.4	The deflection of free end of the cantilever models under loading	124
Table 4.5	The actual deflection at free end before white-painted	128
Table 4.6	The actual deflection at free end after white-painted	134
Table 4.7	The difference and standard deviation of the deflection profiles before and after painting	135
Table 4.8	The comparison of the measurement results obtained from <i>Alicona</i> System and PSSM	137
Table 4.9	The bending modulus calculated from the deflection results obtained from <i>Alicona</i> and PSSM method	138
Table 4.10	The bending modulus of the epoxy coated PET cantilever	145
Table 4.11	The displacement results of reinforced-epoxy coated PET micro-cantilever with load of 0.1 N	149



Table 4.12	The Gradient of the deflection curves	151
------------	---------------------------------------	-----

## LIST OF FIGURES

		<b>Page</b>
Figure 2.1	The optical layout for optical interferometric technique	14
Figure 2.2	The Mireau interference objective technique	15
Figure 2.3	Schematic diagram of the phase shifting shadow moiré setup	18
Figure 2.4	The experimental setup for ISDG	23
Figure 2.5	Schematic of the ISDG	24
Figure 2.6	Experimental setup for optical interferometry	26
Figure 2.7	Fringe pattern on a micro beam in an accelerometer	26
Figure 3.1	Schematic of the copper cantilever with unknown bending modulus	40
Figure 3.2	A typical design of an accelerometer. (a) The isometric view (b) The detail dimensions of the accelerometer	41
Figure 3.3	The schematics of the steps in the fabrication process. (a) Cross section A-A of the accelerometer. (b) The side view of the cross section A-A and a series of fabrication steps	45
Figure 3.4	Flow chat for the fabrication process of silicon micro-cantilever	47
Figure 3.5	The top and the bottom mask plotted in the negative form. (a) Top mask. (b) Bottom mask	47
Figure 3.6	(a) The schematic diagram of the wafer and the cutting lines (b) One of the four piece wafer after cutting	48
Figure 3.7	The Surface Optical System Filmatrics thin layer measurement equipment	49

Figure 3.8	The wafer after the wet oxidation process	50
Figure 3.9	The successful photo-resist development	50
Figure 3.10	The image of the wafer after the silicon dioxide at the open windows is removed	51
Figure 3.11	(a) The etching process using KOH 25% at temperature 75°C. (b) The bottom surface of the wafer after first KOH etching	52
Figure 3.12	The patterned photo-resist layer on the top surface of wafer	53
Figure 3.13	The image of the accelerometer structures after the second etching	54
Figure 3.14	The serious over etching of the wafers. (a) The serious over etching at the top surface of the wafer. (b) The serious over etching at the bottom surface of the wafer	54
Figure 3.15	The SEM photo for the fabricated cantilever. (a) The top view of the cantilever. (b)The side view of the cantilever and measurement is done at the 20° tilted angle	56
Figure 3.16	The geometry analysis of the actual thickness of the cantilever (cross-section view)	57
Figure 3.17	Sample preparation process for reinforced-epoxy coated PET cantilever	58
Figure 3.18	The specimen prepared. (a) The PET sheet that is coated with various reinforced-epoxy after curing. (b) Part of the specimens of reinforced-epoxy coated PET cantilever. (c) The cross-section view of the 30% graphite-epoxy coated PET cantilever	59
Figure 3.19	The experimental setup for the deflection measurement of miniaturized copper cantilever. (a) Schematic of the copper cantilever with unknown bending modulus. (b) Image of the PSSM setup for copper cantilever deflection measurement	62
Figure 3.20	The experimental setup for the deflection measurement of micro-cantilever	64

Figure 3.21	(a) The undistorted grating with pitch $p$ . (b) The distorted grating with the pitch $p$ and carrying the distortion function $f(x,y)$	66
Figure 3.22	The infinite fringe moiré pattern formed by superimposed the distorted grating with the undistorted grating	68
Figure 3.23	The finite fringe moiré pattern	68
Figure 3.24	Two types of grating orientations, (a) Vertical grating (parallel to $y$ -axis). (b) Horizontal grating (parallel to $x$ -axis)	69
Figure 3.25	(a) Setup for shadow moiré technique. (b) The shadow moiré pattern of a spherical surface	71
Figure 3.26	(a) Moiré pattern with $0 \pi$ phase-shifted. (b) $2/3 \pi$ phase-shifted. (c) $4/3 \pi$ phase-shifted. (d) The phase map after applying phase-shifting algorithm. (e) The reconstructed surface profile after applying phase-unwrapping algorithm	77
Figure 3.27	The illustration of terms $a$ , $b$ , $I_{max}$ and $I_{min}$ in fringe pattern	78
Figure 3.28	The cantilever loaded with a point load at the free end	80
Figure 3.29	The schematic of the bending condition of the cantilever. (a) The top view of the cantilever. (b) The loads applied to the cantilever (side view)	82
Figure 3.30	An image of Ronchi ruling that captured to determine the scaling factor of the imaging system. (a) The entire image. (b) The magnified area of Ronchi ruling that consists of 10 line pairs	84
Figure 3.31	The flowchart of the various stages of the PSSM in deflection measurement of the copper cantilever	86
Figure 3.32	The flowchart of the various stages of the PSSM in deflection measurement of the silicon cantilever	87
Figure 3.33	<i>Alicona</i> imaging system. (a) The image during the measurement. (b) The image of loading jig during experiment	89
Figure 3.34	The meshed cantilever models. (a) The cantilever model that is meshed with SHELL91 element. (b) The cantilever model that is meshed with SOLID46 element	94

Figure 3.35	The displacement results. (a) The displacement result for the single layer shell element model. (b) The displacement result for the single layer solid element model	95
Figure 3.36	The displacement results. (a) The displacement result for the double-layer shell element model. (b) The displacement result for the double-layer solid element model	97
Figure 3.37	The model of the Reinforced-epoxy coated PET micro-cantilever	99
Figure 4.1	The 0 radian phase shifted image of the cantilever after loading	102
Figure 4.2	The result of deflection measurement of miniaturized copper cantilever. (a) The 0 $\pi$ radian phase-shifted fringe pattern. (b) The $2\pi/3$ radian phase-shifted fringe pattern. (c) The $4\pi/3$ radian phase-shifted fringes pattern. (d) The wrapped phase-map. (e) The unwrapped phase map. (f) The deflection profile at section A–A, B–B and C–C	104
Figure 4.3	The deflection of miniaturized copper cantilever. (a) The profile before loading. (b) The profile after loading. (c) The comparison of the profile before and after loading. (d) The deflection profile obtained from PSSM (after subtraction) and the profile obtained from theory ( $E=60.65$ GPa)	105
Figure 4.4	The schematic of the cylinder profile and the location of the data points	108
Figure 4.5	The analysis area of the cylinder measured	109
Figure 4.6	The cylinder profile measurement results. (a) The 0 $\pi$ phase-shifted image. (b) The $2/3 \pi$ phase-shifted image. (c) The $4/3 \pi$ phase-shifted image. (d) The wrapped phase map. (e) The unwrapped phase (3-D representative). (f) The measured and theoretical cylinder surface profiles at the section A–A	111
Figure 4.7	(a) The measurement result from profile projector compared with theoretical value. (b) The phase-shift shadow moiré result compared with the profile projector result. (c) The curve fitted phase-shift shadow moiré result compared with the profile projector result	113

Figure 4.8	The low contrast fringe patterns of the silicon micro-cantilever after loaded with point loads. (a) Moiré fringes on the silicon cantilever after it is loaded with 0.0257N load. (b) The fringe pattern of the cantilever after loaded with 0.0368 N load	116
Figure 4.9	The intensity enhancement of poor contrast image. (a) The histogram of the analysis area shown in Figure 4.8(a). (b) The intensity profile of section A–A in the original image. (c) The intensity profile of section A–A after contrast enhancement. (d) The intensity profile of section A–A after contrast enhancement and averaging filtered	119
Figure 4.10	The measurement results for silicon micro-cantilever using PSSM method: (a), (b) and (c) are the original images with $0\pi$ , $2\pi/3$ and $4\pi/3$ phase shifted, (d), (e) and (f) are the images from (a) to (c) after contrast enhancement, (g) the phase map, (h) the three-dimensional representative (unwrapped phase), (i) the deflection profile for section A-A before and after loading (0.0257 N), (j) the actual deflection profile for the applied loads of 0.0257 N and 0.0368 N respectively	122
Figure 4.11	(a) The image of silicon micro-cantilever before white-painted and before loading. (b) The image of silicon micro-cantilever before white-painted and after loading	126
Figure 4.12	The surface profiles and deflection profiles measured (before painted). (a) The surface profile of silicon cantilever before loaded. The surface profile measured after loaded with load 0.0257N. (c) The actual deflection profile obtained from subtraction of surface profiles before and after loading	127
Figure 4.13	The actual deflection profile (before painted) measured by the load of 0.0368N	128
Figure 4.14	The image of the micro-cantilever after white painted	129
Figure 4.15	The paint thickness and the distribution of the white paint on the surface of cross-section A-A	130
Figure 4.16	(a) The image of silicon micro-cantilever after painted and the before loading. (b) The image of silicon micro-cantilever after painted and after loading with 0.0257N load	131
Figure 4.17	The deflection profile after white-painted. (a) The surface profile	

	of silicon micro-cantilever before loading. (b) The surface profile measured after loading with load 0.257 N. (c) The actual deflection profile obtained from subtraction of surface profiles before and after loading	133
Figure 4.18	The actual deflection profile (after painted) for the load of 0.0358N	134
Figure 4.19	The comparison of deflection profile before and after painting. (a) The deflection profile using the 0.0257 N load. (b) The deflection profile using the 0.0368 N load	136
Figure 4.20	(a) The analysis area of the 30% graphite-epoxy coated PET cantilever. (b) The low contrast fringe patterns and the corresponding irregular phase-map. (c) The phase-shifted images after contrast enhancement and the corresponding phase-map before loading. (d) The phase-shifted images after contrast enhancement and the corresponding phase-map after loading	140
Figure 4.21	(a) Three-dimensional surface profile before loading. (b) The three-dimensional deflection profile after loading. (c) The actual deflection profile after subtraction of the profiles before and after loading	142
Figure 4.22	Graph of deflection versus distance along cantilever. (a) Two-dimensional plots of profile before loading, after loading and the actual deflection profile, (b) The comparison of the deflection profile plotted from the measurement and the theoretical	143
Figure 4.23	Comparison of the bending modulus between the aluminum-epoxy coating and the graphite-epoxy coating on PET cantilever	145
Figure 4.24	The deflection of the 30% graphite-epoxy coated PET cantilever. (a) The contour plot of the deflection. (b) The comparison of deflection results from experimental and FEA	148
Figure 4.25	The trends of the deflection at free end of reinforced-epoxy coated PET micro-cantilever when the thickness of coatings increased. (a) The trends of the deflections for various types of aluminum-epoxy coatings. (b) The trends of the deflections for various types of graphite-epoxy coatings	150

Figure 4.26 The deflection gradient of the various types of reinforced-epoxy  
PET cantilever

152

### **LIST OF ABBREVIATIONS**

2-D	– Two-dimensional
3-D	– Three-dimensional
CCD	– Charge coupled device
FEA	– Finite element analysis
MEMS	– Micro electro-mechanical system
PET	– Polyethylene terephthalate
PSSM	– Phase-shift shadow moiré

## **LIST OF APPENDICES**

- Appendix A – Dimensions of the silicon accelerometer
- Appendix B – The detail description of the sample preparation steps
- Appendix C – The processing algorithm for deflection measurement
- Appendix D – The processing algorithm for cylinder profile measurement
- Appendix E – The image enhancement processing algorithm
- Appendix F – The excel spreadsheets to calculate the bending modulus  
and uncertainty
- Appendix G – Analysis of deflection of micro-cantilever that has various thicknesses



**KESAN SALUTAN DIPERKUKUH EPOKSI TERHADAP MODULUS  
LENTURAN BAGI JULUR-MIKRO DENGAN MENGGUNAKAN KAEDAH  
MOIRÉ BAYANGAN ANJAKAN FASA**

**ABSTRAK**

Dalam rekabentuk dan analisis ke atas julur-mikro PET bersalutan diperkukuh epoksi, kegunaan nilai modulus lenturan yang tepat dalam analisis adalah penting. Nilai modulus lenturan yang tepat juga penting untuk mengkaji kesan salutan diperkukuh ke atas julur-mikro ini. Kajian ini bertujuan untuk menggunakan kaedah moiré bayangan anjakan fasa (PSSM) untuk mengukur pesongan julur-mikro PET bersalutan diperkukuh epoksi supaya modulus lenturan bahan salutan boleh ditentukan. Pada mulanya, PSSM dibangunkan untuk mengukur pesongan julur tembaga yang kecil untuk mengkaji kebolehan kaedah ini untuk mengukur pesongan mikro. PSSM kemudian diubahsuai dan dibaiki dengan menggunakan teknik-teknik pemprosesan imej untuk meningkatkan kebolehlihatan pinggir-pinggir moiré yang tidak jelas supaya dapat digunakan untuk mengukur pesongan julur silikon-mikro. Spesimen silikon julur-mikro telah dibentuk dengan menggunakan teknik pemesinan permukaan-mikro. Kaedah PSSM yang lebih baik telah berjaya digunakan untuk memproses corak pinggiran moiré yang tidak jelas dilihat dan dapat memproses data pesongan. Kajian mengenai kesan bahan salutan diperkukuh epoksi kepada julur-mikro PET kemudian dilakukan. Sampel telah dihasilkan dengan cara menyalut salutan aluminium-epoksi dan salutan grafit-epoksi ke atas kepingan PET melalui acuan. Julur-mikro spesimen kemudian dibebaskan dengan cara memotong PET bersama-sama dengan salutannya mengikut corak acuan. Pelbagai jenis salutan

diperkukuh epoksi telah didapati mempengaruhi modulus lenturan julur-mikro PET yang bersalutan. Modulus lenturan didapati meningkat apabila peratusan aluminium dan grafit di dalam epoksi meningkat. Kajian kesan bahan-bahan salutan telah diperluaskan dengan menggunakan analisis unsur terhingga (FEA). Nilai modulus lenturan bahan-bahan salutan yang ditentukan dari kerja uji kaji telah digunakan sebagai parameter kemasukan dalam analisis dan tebal salutan telah diubah-ubah. Siasatan daripada FEA mencadangkan bahawa ketebalan yang sesuai untuk salutan diperkukuh epoksi adalah kira-kira 160  $\mu\text{m}$  hingga 180  $\mu\text{m}$  berdasarkan pada kenaikan keanjalan. Kerja-kerja penyelidikan ini adalah banyak tertumpu kepada penyediaan spesimen dan penambahbaikan kaedah PSSM dengan menggunakan teknik pemprosesan imej, serta kajian kesan salutan pada julur PET. Penyelidikan menunjukkan bahawa kaedah PSSM yang lebih baik mampu untuk mengukur pesongan mikro dengan kesilapan minimum dan modulus lenturan julur-mikro boleh diubah dengan menggunakan bahan-bahan salutan yang berlainan. Tanpa mengubah dimensi utama julur-mikro, modulus lenturan julur-mikro boleh diubah oleh bahan-bahan salutan dan oleh itu, julur-mikro dengan sensitiviti yang berlainan boleh dihasilkan.

**THE EFFECT OF REINFORCED-EPOXY COATING ON THE BENDING  
MODULUS OF MICRO-CANTILEVER USING PHASE-SHIFT SHADOW  
MOIRÉ**

**ABSTRACT**

Applying an accurate bending modulus value of the material is important in the design and analysis of the reinforced-epoxy coated PET cantilevers. This is because the accurate bending modulus value is important in evaluating the effect of the various coatings onto the micro-cantilever. This research is aimed at applying the phase-shift shadow moiré method (PSSM) for the deflection measurement of reinforced-epoxy coated PET micro-cantilevers in order to determine the bending modulus of the micro-cantilever material. The PSSM was initially developed to measure the deflection of a miniaturized copper cantilever and the feasibility of the method was studied to measure micro-deflection. The PSSM was then modified and improved using image processing techniques to enhance the poor visibility moiré fringes before applying it to measure the deflection of a silicon micro-cantilever. The silicon micro-cantilever specimen was fabricated using surface micro-machining technique. The improved PSSM method was successfully applied to process poor visibility fringe patterns and deflection data was extracted. A study on the effect of different coating materials in the reinforced-epoxy coated PET micro-cantilever was then carried out. The samples were fabricated by applying the aluminum-epoxy and graphite-epoxy coatings on PET sheets through a mold. The micro-cantilevers specimens were then released by cutting the PET with coating according to the patterns of the mold. The various types of the reinforced-epoxy coatings were found

to affect the bending modulus of the coated PET micro-cantilevers. The bending modulus increased as the percentages of the aluminum and graphite reinforcement in the epoxy increased. The study of the effect of the coating materials were extended by using the finite element analysis (FEA). The bending modulus values of the various types of coating materials determined from experimental work were applied as the input parameter and the thickness of the coatings were altered. The investigation from the FEA suggested that the optimum thickness of reinforced-epoxy coating is about 180  $\mu\text{m}$  based on the increment of the stiffness. The research work was focused on the specimen preparation and improvement of the PSSM method with image enhancement technique, as well as the study of the effect of the coating on PET cantilever. The research shows that the improved PSSM method is capable of measuring the micro-deflection with minimum error and the bending modulus of the micro-cantilever can be altered by using different coating materials. Without changing the major dimensions of the micro-cantilever, the bending modulus of the composite cantilever material can be varied and therefore micro-cantilevers with different sensitivities can be produced.

# CHAPTER 1

## INTRODUCTION

### 1.0 Research background

Micro-electro mechanical systems (MEMS) consist of two major components, which are the sensing (actuating) element and the signal transduction unit. MEMS are widely applied for various applications, such as microwave and RF communications, optical networking, and acoustic and mechanical sensors. In the context of mechanical sensors, MEMS sensors have been adopted by industries to produce airbag sensors, various types of pressure sensors, AFM probe tips and micro-engines. MEMS sensors are more versatile than the conventional sensors and, thus, have become popular due to multiplicity, microelectronic and miniaturization (Wang et al., 2003).

Most of the MEMS sensors contain small plates, diaphragms, bridges or cantilevers that are either made from or coated by piezo resistive material in the size scale of micrometers (Arivindran, 2007). These components respond to mechanical loads, such as force and pressure, by means of out-of-plane deflection. The deflection produces the piezo-resistive effective, thus converting the mechanical stress into electrical signal. The conversion of mechanical stress into electrical signal is essential to enable the integration of MEMS sensors with microelectronic circuits.

Since the out-of-plane motion of cantilever beam or diaphragm is usually critical to MEMS sensors operation, the accurate measurement of these small movements is essential to characterize the behavior of the sensor under load.

Although, significant effort has been put into the development of improved MEMS design and fabrication processes, research of MEMS measurement and testing have received less attention, especially the measurement of mechanical properties. For example, in an accelerometer that deploys an air bag during a car crash, it is fundamental importance to measure accurately the mechanical behavior and properties of the micro beam.

In the design of MEMS sensors and actuators the design parameters such as dimensions are dependent upon the extreme operating conditions and the mechanical properties of the materials used. Another important design consideration is the maximum allowable deflection of the structure such as micro-cantilever beam. The micro-cantilever should deflect within a range to ensure safety and accuracy, thus preventing yielding and fatigue failure. Therefore, in order to ensure the correct design, the maximum deflection and the mechanical properties of the MEMS structures have to be determined a priori. The above mentioned problems are usually solved by using finite element analysis (FEA).

The predictions of the FEA depend largely on the assumptions made during the generation and analysis of the model. Researchers tend to model the MEMS structures such, as cantilever beams or diaphragms, using the standard value of mechanical properties such as Young's modulus as the FEA input parameter. However, like many other properties, the mechanical properties of micro-structures deviate from the bulk materials due to the small dimensions of the micro-structures (Son et al., 2003). The standard value of Young's modulus for the bulk material may not be applicable to micro-system such MEMS cantilevers and diaphragms. This is

because the specimen size effect of the mechanical properties at micro-scale range is critical. In some polymer-based MEMS, the micro-structures are normally reinforced composites or multi-layer coated composites in which the mechanical properties differ from the standard values. In such situations, the use of the standard value of mechanical properties for FEA will lead to the wrong prediction of the deflection under load. Therefore, the only way to determine the correct value of mechanical properties of micro-scale structures is by conducting experiments.

Only the direct and accurate measurement can ensure the actual value of the deflection and mechanical properties for MEMS. However, accurate measurement of the deflection profiles of micro-structures, such as micro-cantilevers, is difficult using conventional point-wise contact methods. This is because the probe of the measurement device will impose additional loads on the micro-structure, thus contributing to significant measurement errors. Optical measurement methods such as holographic interferometry (HI), electronic speckle pattern interferometry (ESPI), fringe projection, shadow moiré and moiré interferometry are well known as reliable, accurate, non-contacting and non-destructive methods for measuring surfaces. The non-contacting nature of these optical methods is an important and essential element in the measurement of the micro-structures.

Among the optical methods, shadow moiré is a well known and widely used measurement technique used for out-of-plane deformation measurement. This method is preferable because the experimental setup is relatively simple compared to other optical methods. The shadow moiré method also has an advantage over other optical method because the measurement range and sensitivity can be easily

controlled. The shadow moiré technique is versatile and the phase-shifting technique can be integrated with shadow moiré method in order to enhance the measurement resolution.

The silicon-based materials have been widely used in the fabrication of many mechanical structures in MEMS (Firebaugh et al., 2004). The widely accepted application of the silicon-based materials in MEMS are mainly because the mechanical structures can be fabricated using surface micro-machining technique (Cho, 2009) and the silicon-based structures are easy to be integrated with electronic circuits. With the improvement of the fabrication technology such as polymer-based micro-machining technique (Nguyen & Huang, 2006) of the polymeric materials, it is possible to fabricate the MEMS structures using polymer-based materials. The significant advantages of polymer-based MEMS over the silicon-based MEMS are that the polymers are ductile but have high impact resistance, flexible, and moreover, the elasticity modulus can be easily altered by using fillers, reinforcement or coatings. Some polymer-based MEMS structures are non-hazardous and non-reactive to most of the chemicals and, thus, can be applied in many biomedical devices such as the micro-cantilever in a micro-pump system.

The amorphous type of polyethylene terephthalate (PET) has the advantages of high impact-resistance, lightweight and good flexibility. When fabricated in the biaxially oriented thin film form, the PET film has a high strength-to-weight ratio and high flexibility. As such, the PET film is often used in applications such as flexible food packaging, thermal insulation and tape applications, such as the carrier for magnetic tapes and backing for pressure sensitive adhesive tapes. PET has



relatively low elasticity modulus which is 50 to 100 times lower than that of silicon (Nguyen & Truong, 2004). Thus, PET micro-cantilevers are more sensitive compared with silicon. Furthermore, PET micro-cantilever can be coated with various materials to alter the Young's modulus.

In the fabrication of the polymer-based MEMS cantilever, the bending modulus of the MEMS cantilevers can be altered by using the different thick-coating materials. The major reason to alter the bending modulus of the cantilevers is to produce the flexible micro-cantilever with different sensitivity with respect to loading, without changing the major dimensions of the micro-cantilevers. The altered bending modulus has to be determined from the deflection measurement in order to facilitate the design and fabrication of MEMS. The shadow moiré method is a promising method to be applied to measure the deflection of the micro-cantilever.

### **1.1 Motivation of the study**

This study is motivated by the need to find an accurate measurement method for the deflection measurement of the polymer-based MEMS micro-cantilever so that the bending modulus of the coated PET micro-cantilever can be determined. An accurate experimental method to measure the deflection should be developed, and the accuracy of the measurement method has to be established.

The study on the effect of different coating material for the PET micro-cantilever is also desired because the knowledge of altering the bending modulus of the reinforced-epoxy coated PET micro-cantilever can facilitate in the design and

applications of this polymer-based MEMS. The results from the finding of the bending modulus of the various reinforced-epoxy coated PET cantilevers provide the actual input parameter to the FEA in the design and fabrication process. The effect of the types and coating thickness is a desired outcome of the FEA.

## **1.2 Problem statements**

The design and analysis of the reinforced-epoxy coated PET cantilever need the accurate value of bending modulus. The effect of the coating materials to this composite micro-cantilever can only be evaluated by knowing the accurate bending modulus of the cantilever materials. The effect of the various coating materials and thicknesses play an important role in terms of cantilever deflection. The evaluation of the effect of the various coatings can facilitate the design and fabrication of this type of composite micro-cantilever.

The conventional point-wise testing method such coordinate measurement machine cannot be applied to determine the accurate bending modulus due to the small dimensions of the micro-structure. Shadow moiré method is a promising non-contact method to measure the deflection and the bending modulus can be calculated from deflection results. However, the uses of the normal light source in the simple experimental setup introduce significant errors. The fringe pattern produced from shadow moiré needed to be improved and the phase-shifting analysis technique needed to be to be integrated in the fringe analysis so that the accurate deflection and bending modulus of the reinforced-epoxy coated PET micro-cantilever can be determined.

### **1.3 Objectives of study**

Based on the above mentioned motivation and problem statements, the objectives of the study are determined as:

- i. To develop a non-contact measurement technique to measure the deflection of micro-cantilevers using phase-shift shadow moiré method (PSSM).
- ii. To determine the bending modulus of the cantilever material through the measurement of the deflection of the silicon micro-cantilever.
- iii. To determine the corresponding bending modulus of the various types of reinforced-epoxy coated PET cantilever through the measurement of the deflection of the cantilever.
- iv. To study the effect of the various coating materials and coating thickness on the stiffness and deflection sensitivity of the coated PET cantilever through the FEA by applying the bending modulus determined experimentally as the input parameter.

### **1.4 Scopes of study**

The study is limited to the following aspects:

- i. The experimental setup of the shadow moiré is developed from the fundamental theory of the shadow moiré method. The arrangement of the equipment is simple and uses the normal visible light source.
- ii. The processing algorithm to enhance the image quality and the phase-shifting algorithm are written in the MATLAB programming language.
- iii. The silicon micro-cantilever is fabricated to test the accuracy and reliability of the developed PSSM technique by comparing the deflection measurement results

with the results from a commercially available equipment namely, *Alicona Imaging System*.

- iv. The reinforced-epoxy coating materials are aluminum-epoxy coating and graphite-epoxy coating. These two types of coating will applied onto the PET cantilevers to create the reinforced-epoxy PET cantilevers.
- v. The models of reinforced-epoxy coated PET cantilever are created and analyzed using the ANSYS software.

## **1.5 Contributions**

Upon completion of this research, three major contributions are expected:

- i. The development of a relatively simple measurement method to measure micro-deflection of MEMS cantilever.
- ii. The effect of various coating on PET polymer-based micro-cantilever is figured out and the knowledge can help in the design of epoxy coated PET micro-cantilever.
- iii. The experimental results and bending modulus found can be used as input parameter to evaluate the effect of coating and the data obtained can facilitate the design and fabrication of reinforced-epoxy coated PET cantilevers.

## **1.6 Thesis outline**

This thesis consists of five chapters that include the Introduction, Literature Review, Methodology, Results and Discussions, and also Conclusions and Future works. The first chapter presents an overview of the research. The background of the

problems is discussed and the objectives of the research are listed after the discussion of the motivation of study. The contributions of this research are highlighted and the thesis outline is included in the last sub-chapter in Chapter One.

Chapter Two in this thesis discusses the literature reviews and the works done by other researchers regarding the research problem. The discussions in this chapter are focused on the application of the optical techniques in deflection measurement, especially the application of moiré method. The characterization technique used in characterization of micro-structures, the research in polymer-based micro-cantilever, and the application of FEA in designing micro-structures are also reviewed. A discussion and comment on the previous works done is presented in the chapter summery at the end of the chapter.

The detail research methodology is discussed in Chapter Three. All the major supporting theories including the shadow moiré method, phase-shifting algorithm and the deflection theory are thoroughly discussed. Next, the procedures of the experimental specimens are outlined. The specimens prepared including the miniaturized copper cantilever, the silicon micro-cantilevers and the reinforced epoxy coated PET cantilevers. After specimen preparation, the experimental setup for the above mentioned specimens are illustrated. The FEA pre-processing procedure for deflection prediction is also presented in this chapter. A brief chapter summary is included.

The experimental results and discussions are compiled in Chapter Four. The experimental results for the copper mini-cantilever, silicon micro-cantilever and the

reinforced-epoxy coated PET cantilever are illustrated and discussed respectively. The bending modulus found from the experiment of reinforced-coated PET cantilever is applied in the FEA to simulate the deflections and evaluate the effect of the various coatings. The conclusions are presented according to the discussions and are compiled in Chapter Five. The contribution of the research, the limitation and the future works are included. The possible extended research areas are suggested.

## **CHAPTER 2**

### **LITERATURE REVIEW**

#### **2.0 Overview**

This chapter presents the review of previous works done regarding the following areas of researches:

- The application of optical techniques in deflection measurement.
- The characterization technique for micro-structures
- The application of polymer materials in MEMS
- The application of FEA in the analysis of MEMS
- The effect of coating to the material properties of MEMS structures

At the end of this chapter, a chapter summary regarding the above mentioned literatures is presented.

#### **2.1 The application of optical techniques in deflection measurement**

Optical metrology is categorized as a non-destructive testing (NDT) and also non-contact measurement method. The purpose of NDT is to determine whether or not a component has a fault without causing material damage during the process of test (Jones & Wykes, 1989). Optical techniques are suitable for MEMS measurement since they are non-contacting and can detect surface displacement that result from the application of small loads. According to Sciammarella (2003), the optical techniques are based on the concept of interference of light. Loads either mechanical or thermal are applied in such a way so that it causes the displacement of object surface and the displacement causes the interference of wave front. The interference

will form a carrier of signal which is known as a fringe pattern on the object surface. The fringe pattern is then analyzed by using manual analysis or automatic processing technique and hence enables measurement to be made.

There are several optical methods can be applied to measure displacement of an object surface, i.e. moiré interferometry, shadow moiré, holographic, speckle photography, speckle interferometry, numerical correlation of speckles, speckles shearography, fringe projection and miscellaneous (Sciammarella, 2003; Lim et al., 2003). In general, holographic and speckle pattern interferometry methods are suitable for both in-plane and out-of-plane strain, stress and displacement measurements (Jones & Wykes, 1989). Moiré interferometry is sensitive to in-plane strain, stress and displacement measurements (Kafri & Glatt, 1990). In contrast, shadow moiré, optical interferometry and speckles shearography are more suitable for out-of-plane displacement, deformation and surface profiling measurements (Gasvik, 1996; Shang et al., 2000). There are many published works on the application of optical metrology since the first invention of interferometer by Michelson in the 1870s. However, since deflection of MEMS cantilever is the out-of-plane displacement, the literature review below will only focus on the application of optical methods on MEMS deflection.

Measurement of deflection can be accomplished by mean of measuring and subtracting the surface profile for before and after displacement. Therefore, the techniques that measure deflection or displacement are actually measurement techniques for surface profile. Among the optical methods that can measure deflection, the optical interferometry method has been developed separately by



several researchers in the past due to its high measurement accuracy. Hill et al. (2001) applied the optical surface profiling technique to measure the deformation of a pressure sensor. Wang et al. (2003) applied optical interferometry technique to measure the deflection of the MEMS cantilever in an accelerometer. The methods presented by these two researches were based on the interference of light beams of equal path difference, which results in fringes of equal thickness.

Figure 2.1 (next page) shows the experimental setup for the interferometric technique proposed by Wang et al. (2003). The monochromatic sodium light source was splitted into two beams, one was directed onto the test specimen (micro-cantilever) and another was directed onto an image plane AB. The light beam which was directed to the micro-cantilever passes through an optical plate and air wedge before reaching. The light was then reflected by the micro-cantilever and travelled back, passing through the air wedge, optical plate and finally reflected to the image plane by the beamsplitter. The function of the air wedge was to produce the optical path difference between the reference surface and the testing surface so that interference occurred. The fringes produced represented the height difference measured from the reference plane which is the backplate of the test specimen.

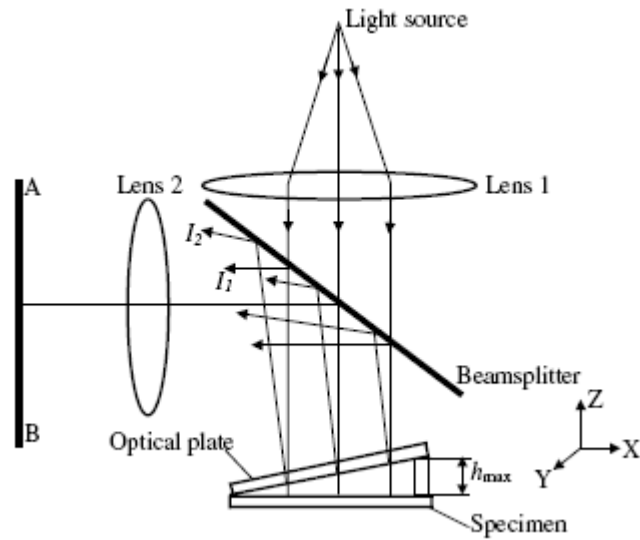


Figure 2.1: The optical layout for optical interferometric technique (Wang et al., 2003).

Later, Wang and Tay (2006) improved the optical interferometric technique by introducing interference Mireau objective based on Michelson interferometer to measure the surface contour map. The experimental technique proposed was based on optical interferometric technique but improved by the Mireau interference objective. Figure 2.2 (next page) shows the Mireau interference objective technique. The Mireau interference objective consisted of an objective lens, a reference mirror and a beamsplitter. The focal length of the objective lens and the mirror were positioned and controlled by computerized piezoelectric device, so that the phase-shifting can be applied. The interferometry technique proposed has high measurement accuracy, low measurement error and flexible. However, the limitations of this technique are that the high intensity laser light source is required and the measurement range is limited by the wave-length of the laser.

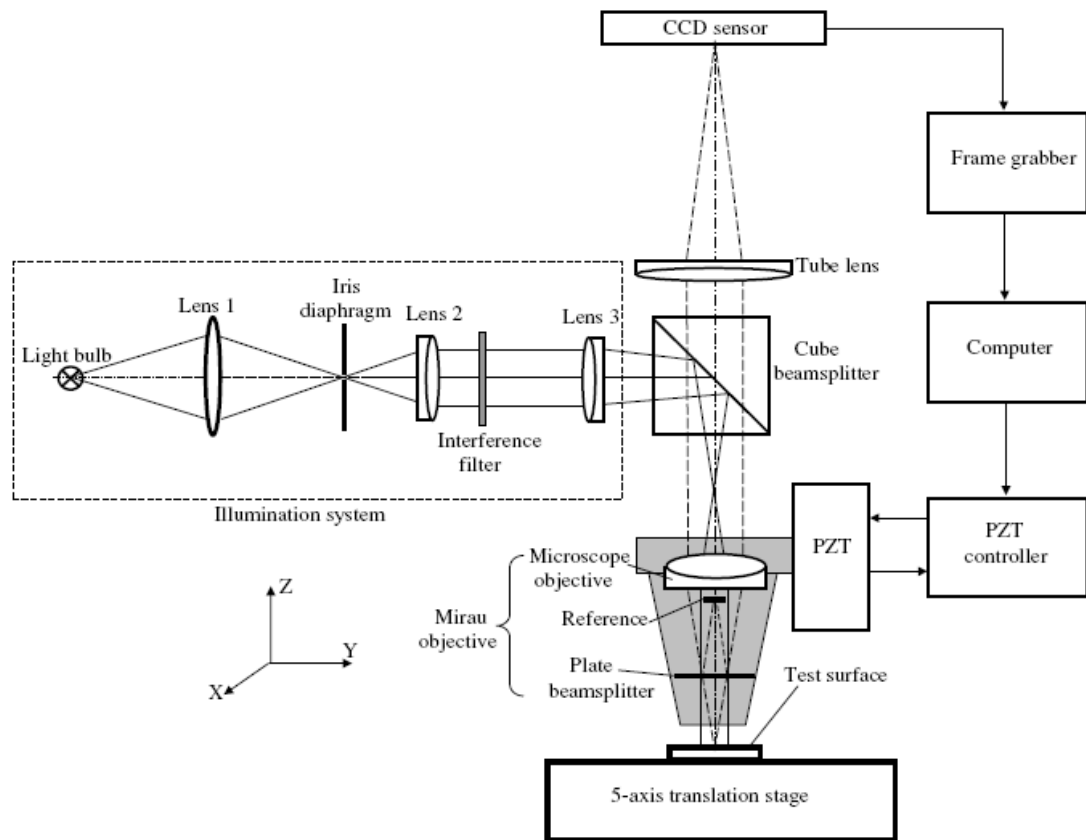


Figure 2.2: The Mireau interference objective technique (Wang & Tay, 2006).

The moiré method is another widely applied method for out-of-plane measurement. The use of the grating in moiré method distinguishes it from others optical metrology (Kafri & Glatt, 1990). One of the attractive features of moiré method is that the resolution of the fringe pattern can be controlled by varying the pitch value of the grating. This method can be roughly divided into moiré interferometry and moiré topography. Moiré interferometry technique is also widely applied to measure in-plane displacement. Recently, researchers have integrated the moiré interferometry technique with phase-shifting interferometry and phase-unwrapping algorithm. This technique is called phase-shifting moiré interferometry and is capable of providing analysts and designers with detailed displacement and strain fields near discontinuities in the composite materials. Perry (1996) has used

this technique to investigate the delaminations in carbon-epoxy/epoxy composites. He proved that this technique allows high resolution measurements of in-plane surface displacements to be made without introducing global smoothing errors, thus preserving the integrity of data near cracks, discontinuities and material interface. However, the phase-shift moiré interferometry is not suitable for deflection measurement of MEMS structures.

On the other hand, moiré topography in particular is a widely used mainly for shape contouring of three-dimensional objects. In general moiré topography can be classified into two main categories; that are projection moiré and shadow moiré, according to the methods of producing moiré fringes. Moiré technique is the technique that utilizes two gratings to generate fringes for the out-of-plane displacement measurement and the measurement resolution can be changed by changing the resolution of grating. Shadow moiré uses one grating as the reference grating and the second grating is actually the shadow of the reference grating that fall onto the object surface. Superimposing of the reference grating with its shadow will form the shadow moiré fringes (Lim, 2003).

The difference between projection and shadow moiré is that two different gratings are used in projection moiré. The difference of the grating can be the difference in the geometry or resolution of the two gratings used. The reference grating is normally projected onto the distorted specimen grating to form the moiré fringes. The projection of the grating can be accomplished by physical projection of grating or can be the virtually superimposing by the aid of the computer programming. Liu & Chen (2005) applied the digital phase-shifting projection moiré

and the wavelet transformation method to measure the deformation of PMMA cantilever beam.

Shadow moiré technique is only sensitive to out-of-plane displacement and is widely applied to measure the deformation and fatigue damage of composite materials. Degrieck et al. (2001) used the digital phase-shift shadow moiré technique to measure micro fatigue damage in reinforcement-reinforcement composite materials. They showed that during fatigue life of a bended specimen, damage was growing steadily and the out-of-plane displacement profile was severely changing. The main advantage of the technique proposed was that only one image was captured and phase shifting was done numerically. Degrieck et al. (2001) concluded that digital phase-shift shadow moiré technique is very efficient and can eliminate all causes of erroneous measurements due to the miscalibration of phase-stepping devices.

Figure 2.3 shows a schematic diagram of the phase shifting shadow moiré setup. Chen et al. (2004) used the phase-shifting shadow moiré techniques to measure wafer curvature and calculate the residual stress. Wafer curvatures or bows can be achieved by analyzing the moiré fringe patterns and film stress can be obtained. As shown in Figure 2.3, the reference grating was located above the wafer. Shadow grating was generated on the surface of the wafer due to the presence of the light source. The CCD camera then records the image of the fringes surface. The reference grating is then moved by  $1/3$  fringe spacing by adjusting the translational positioner. The second image is recorded. The final image was again recorded by moving further  $1/3$  fringe spacing. The images were then processed by using image

processing technique and the surface profile can be calculated based on particular equations. The wafer curvature was then calculated from the surface profile using Stoney's equation (Chen et al., 2004).

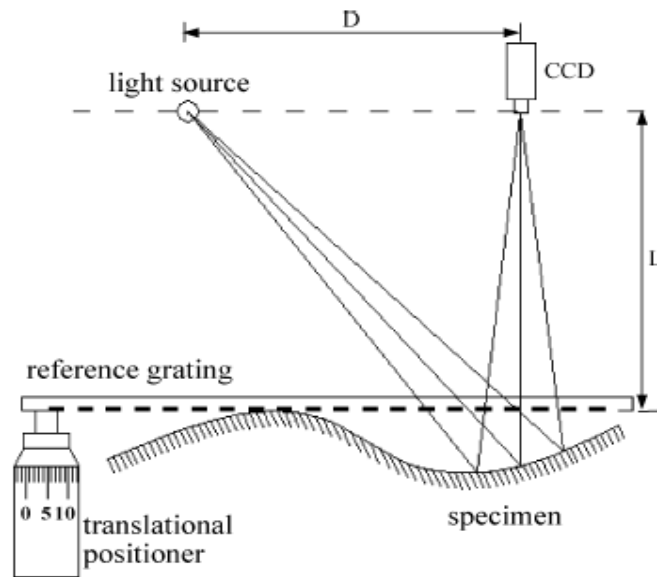


Figure 2.3: Schematic diagram of the phase shifting shadow moiré setup (Chen et al, 2004).

Shadow moiré is also popular in the warpage measurement of printed circuit boards (PCB) (Geng et al., 2006; Wen & Ku, 2008). This technique becomes popular in the PCB warpage measurement is because the measurement range and sensitivity can be easily controlled by changing the resolution of the grating. High-resolution grating produces higher measurement sensitivity. The high temperature during the reflow process and the mechanical preload during the assemble process were contributed to the warpage of PCB. Shadow moiré can provide the real time monitoring of warpage and can be the powerful tool to evaluate the effect of processing parameters to the PCB warpage.

The features that can produce the real time moiré fringes and the flexible measurement range are the major advantages of shadow moiré technique. Seif et al. (2007) made use of these features and applied the shadow moiré laser based imaging technique to study the delamination damage of carbon-epoxy composites after drilling process. The hidden delamination during the drilling process was revealed and the drilling process parameters were evaluated by shadow moiré laser based imaging technique. The shadow moiré technique was also successfully applied in other applications such as shape measurement (Siddiolo et al., 2008), and the mechanical characterization applications that will be discussed in the following section. Table 2.1 summarizes the major features of the popular optical metrology methods that are applied to measure displacement.

Table 2.1: The major features of some popular optical methods applied for displacement measurement.

<b>Optical Method</b>	<b>Light Source</b>	<b>Measurement Types</b>	<b>Major Features</b>
Optical Interferometry	Laser or monochromatic light	Out-of-plane measurement	<ul style="list-style-type: none"> <li>• High measurement accuracy</li> <li>• High precision</li> <li>• Suitable for small displacement (a few <math>\mu\text{m}</math>)</li> <li>• Fixed measurement range</li> </ul>
Holographic	Laser	In-plane and out-of-plane measurement	<ul style="list-style-type: none"> <li>• High measurement accuracy</li> <li>• High precision</li> <li>• Suitable for small displacement (a few <math>\mu\text{m}</math>)</li> <li>• Fixed measurement range</li> <li>• Complicated setup and measurement procedures</li> </ul>
Speckle Interferometry	Laser	In-plane measurement	<ul style="list-style-type: none"> <li>• High precision</li> <li>• Suitable for small displacement (a few <math>\mu\text{m}</math>)</li> <li>• Fixed measurement range</li> <li>• Produce high noise and poor</li> </ul>

			fringe visibility interferogram
Moiré Interferometry	Laser or monochromatic light	In-plane measurement	<ul style="list-style-type: none"> <li>• High precision</li> <li>• Suitable for small and moderate displacement ( a few hundred <math>\mu\text{m}</math>)</li> <li>• Flexible measurement range</li> <li>• Complicated setup</li> </ul>
Shadow Moiré	Monochromatic light or normal visible light	Out-of-plane measurement	<ul style="list-style-type: none"> <li>• High precision</li> <li>• Suitable for moderate and large displacement ( about <math>10\mu\text{m}</math> up to a few mm)</li> <li>• Flexible measurement range</li> <li>• Simple setup and measurement procedures</li> </ul>

Among the optical method reviewed, moiré method is found to be the relatively simple and cost effective method compared with other optical methods in terms of experimental setup. The moiré method is also found to be more flexible compared with interferometric method. The use of interferometric method to measure the deflection is limited to the wave-length of the monochromatic light source used in the technique. Although very precise, the maximum deflection measured by interferometric method usually does not exceed  $50\mu\text{m}$ .

The shadow moiré method has advantage over the interferometric method because the measurement range can be altered by changing the grating resolution. According to the successful examples illustrated in the literatures, the deflection measured by shadow moiré ranges from a few micrometers to a few millimeters depending on the grating used. The previous works also demonstrated the wide application of shadow moiré method. Shadow moiré method was successfully applied in the various fields of studies, such as, deflection of micro-cantilevers, the



delamination damage after drilling process, film stress characterizations, shape measurement, and PCB warpage detections.

The major limitation of the shadow moiré method is that the high intensity light source is usually needed for the micro-scale measurement. The visibility of the shadow moiré fringes, however, decreased as the resolution of the grating increased. The use of laser in such technique is normally preferred because high-intensity light is essential to produce a sharp shadow of the gratings, particularly for measurement on micro-structures. The use of normal white light source for shadow moiré in micro-deflection measurement is relatively difficult because normal light source produces low visibility fringes. Although the measurement resolution can be enhanced by integrating the phase-shifting technique in fringe pattern analysis, the phase-shifting technique will produce erroneous results if the fringe contrast is too low. Another limitation of using the normal light source is that the moiré fringes are limited to a few fringes only. This is because the light is diffracted when passing the grating, thus produce the poor visibility shadow. Therefore, the displacement should be limited to a small range, in order to avoid poor visibility shadow. Most of the previous researches used the collimated and high intensity laser light source to obtain the acceptable visibility images and to obtain the adequate moiré fringes

## **2.2 The characterization technique for micro-structures**

The standard value of Young's modulus of a thin film is different from the value obtained by deriving from the bulk scaling law because the dimension of the thin film is small (Son et al., 2002). The following Table 2.2 lists the Young's modulus of silicon dioxide materials published by IEEE (MEMSnet, 2010). From

Table 2.2, the value of Young's modulus varies from 57 GPa to 92 GPa depending on the condition and processes to prepare the material. The material properties variation is obvious when the various thicknesses and various crystallographic direction silicon materials are applied in the MEMs structures. Therefore, experimental data to determine the material properties, especially the Young's modulus, is very important when applying those properties in FEA.

Table 2.2: The values of Young's modulus for silicon dioxide material at micro-scale conditions (MEMSnet, 2010).

<b>Young's Modulus</b>	<b>Conditions</b>	<b>References</b>
70 GPa	Value obtained by micro-indentation test for thermally grown SiO <sub>2</sub> film on a silicon<111> wafer.	Thin Solid Films, 283 (1996), p.15
74 GPa	Used for electrothermal Bimorphs	IEEE Micro Electro Mechanical Systems Workshop, Feb 1993, Florida, p.25
75 GPa	Thin film, used in semiconductor fabrication.	IEEE, Micro Electro Mechanical Systems Workshop, Feb 1990, Napa Vally, California, p.174
92 GPa	Sputtered grown film, thickness=0.4 um, values are calculated using electro-statically deflectable membrans and Cr for metallization (thickness of 0.01 um), assuming density of 7200kg/m/m/m & Young's Modulus of 180 GPa for Cr films. The accuracy of Young's Modulus is +- 20%.	IEEE Transactions on electron devices, Vol. ED25, No.10, Oct 1978, p.1249
57 GPa	Thermal-wet grown film, thickness = 0.425 um, values are calculated using electro-statically deflectable membranes and Cr for metallization (thickness of 0.015um), assuming density of 7200kg/m/m/m & Young's Modulus of 180 GPa for Cromium.	IEEE Transactions on electron devices, Vol. ED25, No. 10, Oct 1978, p.1249

The early effort to determine the Young's modulus of micro-cantilever was done by Sharpe et al. (1997). The method used was by applying a tensile test on a two-layer polysilicon specimen of dimensions 4 mm length, 0.6 mm wide and 3.5  $\mu\text{m}$  thick. Optical method, namely interferometric strain/displacement gage (ISDG), was applied to measure the in-plane displacement. The Young's modulus and Poisson's ratio were then calculated using theoretical equations. Figure 2.4 shows the experimental setup for ISDG. The specimen was gripped at both ends and the tensile load was applied by load cell that placed on piezoelectric translator. Two gold lines were deposited on the surface of the specimen during manufacture. The gold lines act as the strain gages and the edges of the gold lines reflect laser beam as shown in Figure 2.5. The reflected laser light interferes with the incident laser beam and forms the fringe pattern. The fringe pattern before and after loading were recorded and strain was calculated based on equations. The Young's modulus, Poisson's ratio and tensile strength for polysilicon were found to be  $169 \pm 6.15$  GPa;  $0.22 \pm 0.011$  and  $1.20 \pm 0.15$  GPa respectively. The limitation of this method is that the gold lines needed to be attached onto the specimen. The significant errors may be introduced if the specimen is in micro-scale.

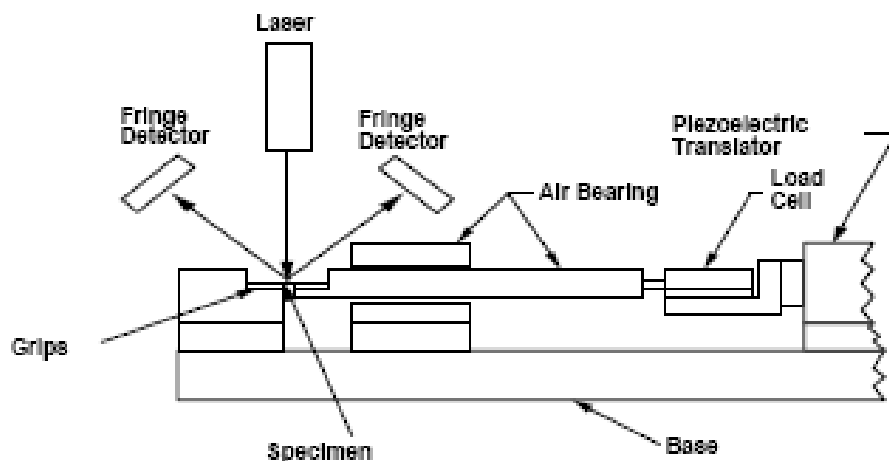


Figure 2.4: The experimental setup for ISDG (Sharpe et al, 1997).

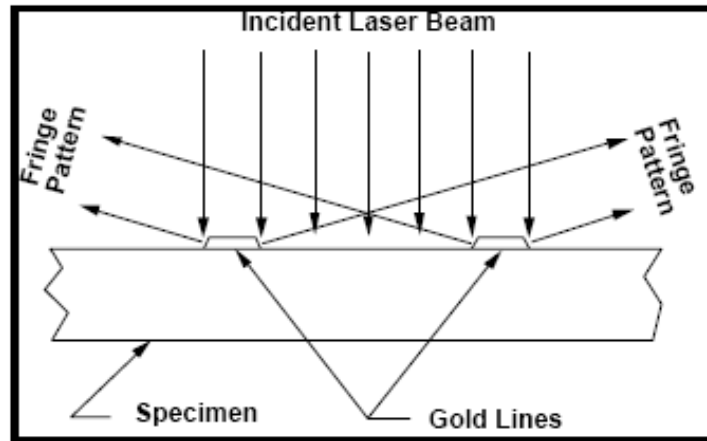


Figure 2.5: Schematic of the ISDG (Sharpe et al, 1997).

The ISDG tensile test method was modified by Zupan et al. (2001) for elevated temperature measurement and later was also used by Cho et al. (2003) to measure Young's modulus of LIGA (an acronym from the German words for lithography, electroplating, and molding) nickel micro-samples of dimensions  $3.7 \text{ mm} \times 1.9 \text{ mm} \times 0.4 \text{ mm}$ . The Young's modulus of the LIGA nickel micro-sample was found to be  $163 \pm 14 \text{ GPa}$ . The major disadvantage of the ISDG tensile test and other tensile testing method is that the test samples are relatively large in dimensions; therefore this technique is difficult to be applied on MEMS cantilever at the actual size.

The bending test is an alternative method to determine Young's modulus especially for materials fabricated in thin strip. For the bending test of MEMS structures, the out-of-plane deflection profiles must be determined using non-contact method. This is because the conventional point-wise method, the probe of the measurement device will impose an additional load on to the micro-structure, thus contributing to significant measurement errors. Wang et al. (2001) applied optical